

<https://doi.org/10.70917/ijcisim-2026-0105>
Article

Art and Design Classroom Driven by Artificial Intelligence: A Study of Teaching Mode Innovation under the Perspective of Multiple Intelligences Theory

Jing Tang *

Communication University of China, Nanjing 211172, Jiangsu, China; jing329084@163.com

Abstract: Based on the theory of multiple intelligences, this paper explores the innovative path of teaching mode driven by artificial intelligence technology. Image processing technology is used to optimize the art design system, and the image brightness equalization and fusion effect is improved by grid chunk repair and wavelet noise reduction. The visual expression sensitivity difference method is introduced to realize high-precision super-resolution reconstruction. Simulation experiments are designed, and the average signal-to-noise removal rate of the proposed system is 56.04% higher than that of the traditional system when the detection time is 100s. The image processing technique proposed in this paper provides better quality input features for subsequent classification tasks by optimizing image brightness equalization and feature fusion. The model shows comprehensive advantages on all types of images, and in the subjective evaluation, it scores 4.67 and 4.78 in both global reconstruction quality and detail reconstruction artistry, respectively, which are better than the control model.

Keywords: art design system; image processing techniques; visual representation sensitivity difference method; super-resolution reconstruction

1. Introduction

Art and design is an extremely interdisciplinary field that integrates and applies knowledge from various disciplines such as society, culture, economics, markets, technology, the Internet of Things, and big data applications [1]. Establishing mechanisms that facilitate interdisciplinary collaboration and integration within the field of art and design is a future trend [2]. The field of art and design essentially reflects the comprehensive qualities of the designer themselves. Due to the extensive interdisciplinary nature of the field but limited class hours, efficiently imparting the aesthetic concepts, design skills, perceptual and cognitive abilities, related scientific and technological knowledge, and market trends through limited classroom instruction remains a key challenge in talent cultivation within the field of art and design [3-6]. At the same time, as the pace of societal change accelerates, art and design disciplines are no longer confined to their narrowly defined cultural, contextual, and historical significance during the creative process. Instead, they are increasingly intertwined with new lifestyle concepts such as smart homes and smart cities, which are transitioning from visionary concepts to tangible realities [7-9]. The integration of intelligent technology-driven design paradigms into art and design disciplines will inevitably catalyze their transformative evolution [10-11]. In response to societal development needs, the demand for enhanced productivity, and the growing reliance on efficient, safe, and intelligent smart home systems and products, this new art design paradigm will inevitably transform traditional art design forms [12-15]. Based on this, the integration of intelligent technology with art education will propel the art design discipline toward a new peak of development, driving artistic advancement toward multidisciplinary convergence with intelligent technology [16-18].

Artificial intelligence (AI) is an emerging technological science that studies, develops, and applies



theories, methods, technologies, and systems aimed at simulating, extending, and enhancing human intelligence [19]. As a key driving force behind the new round of technological revolution and industrial transformation, AI has already made significant strides across various fields, with the art design domain being one of the most important application areas for AI technology [20-22]. On one hand, AI not only mimics the creativity of human artists but also assists designers in creating new forms and styles based on existing works, thereby promoting the deep integration of art and technology. For example, literature [23] indicates that combining generative adversarial models with intelligent algorithms can generate high-quality Pop Art-style images, effectively expanding the expressive forms and style categories of art design, and has been widely applied in the field of cultural and creative product design. Reference [24] proposes an AI-driven Content Style Alignment Module (CSAM), which can match the semantic distribution in content images with style patterns, reducing distortion and deformation during the graphic design stylization process, thereby producing high-quality stylized images suitable for design applications. Literature [25] evaluates the performance of deep learning neural network technology in image design content stylization transfer. The results indicate that this method can effectively transfer the structural and textural information of the input image to the content image, thereby generating high-quality stylized images. Literature [26] leverages deep learning and data mining technologies to deeply explore stylistic features in artistic design, while integrating style suggestions and design optimization methods to provide valuable stylistic information references for artistic designers, laying the foundation for the development of artistic design.

On the other hand, the integration of AI and digital painting has led to profound changes in the artistic creation process, including expression forms, techniques, workflows, and creation cycles. This fusion of technological innovation and creative expression is redefining the boundaries of art. For example, Reference [27] explores the application of artificial intelligence in video art design. Its image generation, video processing, and 3D modeling systems significantly enhance the efficiency of artistic design, making traditional artistic design models more open and diverse. Literature [28] introduces the potential of AI-generated content (AIGC) technology in the aesthetic reproduction and innovative design of furniture. Based on specialized databases and design formulas, it can accurately generate art design paths that meet specific needs, thereby innovating and developing the basic processes of the traditional art design industry. As seen from the above literature, AI's advantage lies in its ability to integrate research and development for simulation, extension, and expansion. Therefore, incorporating AI into art design classroom instruction effectively addresses the limitations of human insight into students' comprehensive theoretical and practical learning, thereby efficiently providing students with more suitable educational content and achieving personalized instruction.

This paper firstly explores the integration path between intelligent technology and art design classroom from a two-dimensional perspective, and takes the course of Plant Landscaping as an example to analyze the logic of the application of intelligent tools and virtual simulation platform in the teaching scenario. Design the art design system which contains two core modules of image processing and super-resolution reconstruction, and optimize the image quality by grid chunk repair, wavelet noise reduction, visual sensitivity difference method and other techniques. Carry out simulation experiments based on Matlab, SPAS/DYEMCT and other tools to verify the effectiveness of the system's image processing module and super-resolution reconstruction module.

2. Art Design Classroom Design Driven by Artificial Intelligence

With the rapid development of artificial intelligence technology and the deepening of the digital transformation of education, the field of art and design education is facing the innovative demand for the integration of the traditional teaching mode and intelligent technology. The theory of multiple intelligences emphasizes the difference and contextualized development of individual intelligence, which provides theoretical support for the innovation of art design teaching mode driven by artificial intelligence. Therefore, the intelligent integration of teaching resources, personalized delivery and precise cultivation of practical ability through technological empowerment has become a key path to break through the bottleneck of traditional classroom.

2.1. Artificial Intelligence + Education

The traditional classroom emphasizes the “teaching” as the center, lecture method, demonstration method, such as traditional teaching methods, teaching content is limited by the teacher's personal teaching experience, knowledge structure, personal style preferences and other subjective factors. Intelligent education will integrate the Internet + big data, the learning content from the books to the screen, the learning place from the classroom to study anywhere.

Taking the “Plant Landscaping” class in environmental art design as an example, at present, most of

the classrooms mainly stay in the traditional mode for plant science popularization, and are relatively weak in combining with artificial intelligence technology. In the classroom, some APP or small plug-ins can be used appropriately to scan the code to recognize plants, through which students can generate strong interest in learning and facilitate the fun of teaching. Secondly, you can develop some software and appropriately use the reward mechanism to stimulate the enthusiasm for learning. These ways of popularization of artificial intelligence science technology in the classroom has a certain degree of dissemination, some focus on the study of plants in the botanical gardens to carry out certain exploration and practice, launched a lot of suitable for us to learn from the APP. for example, Wuhan Botanical Garden of the Chinese Academy of Sciences recently developed a self-service interpretation system based on NFC plant near-field communication, to help tourists to better understand the plants and recognize the plants. Another example is “Flower Companion” and “Shape and Color”, which are similar to the APP developed by Wuhan Botanical Garden, where visitors can get the scientific knowledge of the species by taking photos, which can satisfy the needs of tourists while entertaining them and enhance the overall demand for visiting the botanical garden. Botanical Garden's overall demand for tours.

2.2. Platform + education

The key to virtual simulation training is to establish a sound and perfect rich informationized teaching platform. Teachers should know how to allocate and select appropriate projects, combine the functions, composition and architecture of the virtual simulation training teaching system, select a platform suitable for teaching, and carry out system development, testing and so on. In this study, for the learning task design link, the course is divided as shown in Figure 1 according to the intelligent big data importance screening, also taking “Plant Landscaping” as an example. It can be seen that the course is divided into residential green space, three-dimensional greening, waterfront green space, flower bed plants, flower border planting design, a total of five major categories of course project modules.

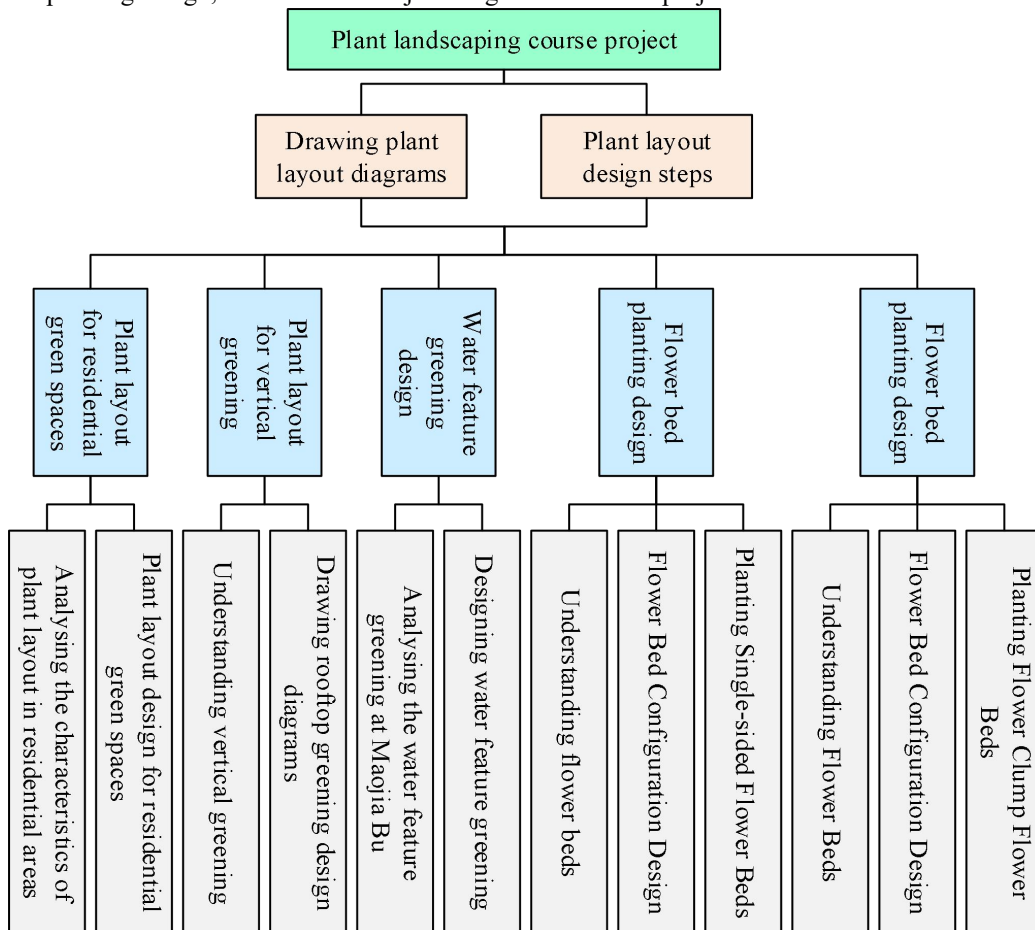


Figure 1. Course Division.

For example, Sketchup2017, EZland software supports this type of development platform and SQL2000 database management system, development and production of educational teaching system platform. The platform needs to include the system administrator module, the teacher module and the

the initial solution vector is $x_{n \times 1}$, and the edge pixel point $\varphi = \theta$ is taken as the center of the restoration localization of the environmental art design image area. Let $\lambda = \sigma / \beta$ and $F = \sqrt{U^2 + V^2}$, the equation of the conduction coefficients of the region of the best matching block is obtained as:

$$h(x, y) = \frac{\lambda}{2\pi\sigma^2} \exp \left[-\frac{1}{2} \left(\frac{x^2}{\sigma^2} + \frac{\lambda^2 y^2}{\sigma^2} \right) \right] \cdot \exp [2\pi j F x'] \quad (1)$$

Choose the minimum error rate ε_i of h_i , determine the visual effect of art design in image restoration by the position of ψ_q^n , compute the interclass bit rate, use the center frequency F as the rotational invariant moment, and the first to-be-restored block to be restored ψ_p as the amount of the center of diffraction, from $\sigma \approx \frac{\pi}{F}$, yielding $F \approx \frac{\pi}{\sigma}$, extracting the broken edges $\partial\Omega$ as well as all the edge pixel points, and denoting the sequence of distributions of the new edge pixel points by the following equation:

$$\phi_n = \frac{\pi k}{N}, k = 0, 1, 2, \dots, N-1 \quad (2)$$

The best matching block window function for the image distribution is obtained by using the confidence finding method for pixel y as $W_i = \sqrt{2}\sigma \approx \sqrt{2} \frac{\pi}{F}$, and the prioritization coefficient adjustment formula for the block to be repaired is:

$$\begin{bmatrix} x' \\ y' \\ 1 \end{bmatrix} = \begin{bmatrix} \cos(-\theta_1) & -\sin(-\theta_1) & 0 \\ \sin(-\theta_1) & \cos(-\theta_1) & 0 \\ 0 & 0 & 1 \end{bmatrix} \begin{bmatrix} x \\ y \\ 1 \end{bmatrix} \quad (3)$$

Where: x, y are the two-dimensional distribution coordinates of the original environmental art design image, respectively. At the broken edge $\partial\Omega$, vector quantization decomposition of adjacent edges is performed inside each sub-block, combined with update iteration to achieve the image brightness equalization repair processing.

3.1.2. Image Fusion and Wavelet Noise Reduction Processing

On the basis of the image brightness equalization processing in art design, combined with the pixel point quantization tracking method for image fusion and wavelet noise reduction processing, in the grid points distributed in the art design image area, it is assumed that the newly extracted art image feature expression equation is:

$$W^{ij}(x, y) = \frac{G^{ij}(x, y)}{\sum_{i=1}^{n_1} \sum_{j=1}^{n_2} G^{ij}(x, y) + \varepsilon} \quad (4)$$

Where: $G^{ij}(x, y)$ is the template distribution centroid moment of the rectangular block with (x^{ij}, y^{ij}) as the fusion region, and the edge contour labeling of the front-view art design image is carried out by pixel labeling to get the extracted edge contour lines noted as:

$$G^{ij}(x, y) = \exp \left\{ -\frac{(x - x^{ij})^2 + (y - y^{ij})^2}{2\sigma^2} \right\} \quad (5)$$

In the design of different 3D geometrical models of art images, the matrix of relevant elements of adjacent blocks is reconstructed for images under different bit shapes such as tilt and rotation, respectively, and the reconstructed pixel point distribution matrix is obtained as:

$$\begin{bmatrix} \cos \theta & -\sin \theta & 0 \\ \sin \theta & \cos \theta & 0 \\ 0 & 0 & 1 \end{bmatrix} \quad (6)$$

Here, the x -axis and y -axis are parallel to the coordinate axes x', y' of the plane where the image is located, and the data item $D(p)$ of the block to be fused is matched with the higher-order feature quantity, and the image noise reduction is carried out under the intensity of the iso-illumination line, and the image noise reduction process is carried out by wavelet reduction technique, and the mother wavelet of wavelet noise reduction is:

$$Q_w(a, b, f) = \sum_{w \in W} c(w) (\lambda(w) Q_0(a, f | w) + (1 - \lambda(w)) Q_0(b, f | w)) \quad (7)$$

Among them:

$$Q_0(x, y) = \frac{\sigma_{xy}}{\sigma_x \sigma_y} \cdot \frac{2\overline{xy}}{\overline{x^2} + \overline{y^2}} \cdot \frac{2\sigma_x \sigma_y}{\sigma_x^2 + \sigma_y^2} \quad (8)$$

$$\lambda(w) = \frac{H(a | w)}{H(a | w) + H(b | w)} \quad (9)$$

denote the scale and weighting coefficients of wavelet noise reduction, respectively, from which the gray level quantization value of the gray level histogram of the art design image in the wavelet primitive vector at $\{(x', y') | x' = 1, 2, \dots, m; y' = 1, 2, \dots, n\}$ is obtained, and for the associated pixel point $X = (x, y)$ in the set of the art design image, the Hennon matrix $H(x, \sigma)$ for obtaining the noise reduction output at the wavelet scale σ is defined as:

$$H(x, \sigma) = \begin{bmatrix} L_{xx}(x, \sigma) & L_{xy}(x, \sigma) \\ L_{yx}(x, \sigma) & L_{yy}(x, \sigma) \end{bmatrix} \quad (10)$$

where: $L_{xx}(x, \sigma)$ is the second-order partial derivative of the one-sample fuzzy edge with respect to $g(x, y, \sigma)$, and $L_{xx}(x, \sigma) = \frac{\partial^2}{\partial x^2} g(x, y, \sigma)$ denotes the localized features of the art design image. The same is true for $L_{xy}(x, \sigma)$ and $L_{yy}(x, \sigma)$.

Gabor filtering is applied to the art design images, and in the reconstructed pixel feature space, the similarity feature representation of different art design specimens is obtained as follows:

$$\begin{aligned} d_i^{k+1} &= (1 - \omega) d_i^k + \left\{ \sum_{j \in N^-(i)} \left(\Theta_i \frac{g_i + g_j}{2} + (1 - \Theta_i) \frac{\Psi'_i + \Psi'_j}{2} \right) d_j^{k+1} \right. \\ &\quad \left. + \sum_{j \in N^+(i)} \left(\Theta_i \frac{g_i + g_j}{2} + (1 - \Theta_i) \frac{\Psi'_i + \Psi'_j}{2} \right) d_j^k - \frac{D_i}{\alpha} \right\} / \\ &\quad \sum_{j \in N(i)} \left(\Theta_i \frac{g_i + g_j}{2} + (1 - \Theta_i) \frac{\Psi'_i + \Psi'_j}{2} \right) \end{aligned} \quad (11)$$

The expressions for $N^-(i)$ and $N^+(i)$ are given below:

$$\begin{cases} N^-(i) = \{j \in N(i) | j < i\} \\ N^+(i) = \{j \in N(i) | j > i\} \end{cases} \quad (12)$$

Establish the gradient information model of the contour distribution of the art design image, and return to the current search path when the signal-to-noise ratio of the noise reduction output image meets the threshold condition, thus completing the noise reduction and image fusion processing of the image in the art design. According to the above image processing results, carry out the optimization design of the

art design system, load the image processing algorithm into the program loading module of the system, carry out the cross-compilation control, and realize the optimization design of the system.

3.2. Image Super-Resolution Reconstruction

In this paper, the introduced visual expression sensitivity difference method is utilized for the processing of image data, which firstly requires the effective calculation of the scanned data information with the formula:

$$(x - x_1) + \Delta x = -f \left(\frac{a_1(x - x_1) + b_1(y - y_1) + c_1(z - z_1)}{a_3(x - x_2) + b_2(y - y_2) + c_3(z - z_2)} \right) \quad (13)$$

where: $f(x)$ that the validity, the general case of the validity is a range of values; x, y, z for the scanning of the image data length, width and height of the digitized. By carrying out the calculation of validity, the data can be stabilized and analyzed, and the stabilized data is once again converted to facilitate the use of the formula:

$$(y - y_o) + \Delta y = -f \left(\frac{a_2(x - x_i) + b_2(y - y_i) + c_2(z - z_1)}{a_3(x - x_2) + b_2(y - y_2) + c_3(z - z_2)} \right) \quad (14)$$

where x, y, z is the effective data's specialization value, which can be transformed by Eq. to directly carry out the calculation of the matching effect.

Each image data has a specific visual expression matching value. The matching value represents the corresponding attribute feature, and the attribute feature coefficient equation is:

$$\begin{cases} \Delta X = X(r^2 k_1 + r^4 k_2) + (r^2 + 2x^2)P_1 + 2xyB \\ \Delta Y = Y(r^2 k_1 + r^4 k_2) + (r^2 + 2x^2)P_2 + 2xyB \end{cases} \quad (15)$$

where: r denotes the integration coefficient; k denotes the attribute extraction coefficient; P is the collocation function; B is the permutation function. To facilitate pixel localization, selected attributes need to be collocated for permutation:

$$\begin{aligned} ML(X, Y) &= |2I(x, x_1) - I(y, y_1) - I(\Delta X, \Delta Y)| \\ F(X, Y) &= \sum_{x=1}^Y \sum_{y=-N}^{J+N} (ML(X, Y) - ML(\Delta X, \Delta Y)) \end{aligned} \quad (16)$$

where: ML is the coefficient value of sensitivity; I denotes the collocation conversion factor. Through the qualification of the conditions, each pixel value with a specific attribute can be determined, and after the determination, the differential calculation can be performed, with the formula:

$$R(i - j) = \frac{\sum_N [f(x, y) \cdot f_1(x, y)]}{\left[\sum_M \sum_N f(x, y) \right]^2 \cdot \left[\sum_M \sum_N f_1(x, y) \right]^2} \quad (17)$$

Difference calculation calculates the pixel values for each frame. The filling of pixels by differential calculation ensures the substantial effect of the artistic image, and the filling calculation formula is:

$$\rho[p(y), q] \approx \frac{1}{2} \sum_{n=1}^m \sqrt{p(y) \cdot q} \quad (18)$$

Substituting Eq. (16) and Eq. (17) into Eq. (18) yields:

$$\rho[p(y), q] \approx \frac{C}{2} \sum_{i=1}^m wk \left(\left\| \frac{y - x}{h} \right\|^2 \right) \quad (19)$$

Organize to get:

$$w = \sum_{n=1}^{\infty} \sqrt{\frac{q}{p(y)}} \delta[b(x) - u] \quad (20)$$

By filling the collation can be obtained about the relationship between the area pixels and the actual design, adjusting the p, q, u adjustment parameter in Eq. (20) can be adjusted for the effect. In order to ensure the accuracy of the position, it is also necessary to carry out the frame rate position establishment, and the formula is:

$$w \begin{bmatrix} x \\ y \\ l \end{bmatrix} = p \begin{bmatrix} x \\ y \\ z \end{bmatrix}, \quad w = 1, 2, \dots, n \quad (21)$$

where: x, y, z is the value of the length, width and height of the area coordinates, which can be adjusted through the transformation of the logical coefficients; the coefficient p is obtained through the actual computation of the formula:

$$p = \frac{\sum_{i=1}^n (G - G_1)(G_1 - G_2)}{\sqrt{\sum_{i=1}^n (G - G_1)^2 (G_1 - G_2)} \cdot \sqrt{\sum_{i=1}^n (G_1 - G_2)^2}} \quad (22)$$

$$E^{LRF}(\phi, f_1, f_2) = \mu \int \frac{1}{2} (|\nabla \phi| - 1)^2 dx \quad (23)$$

The result obtained by Eq. is a coordinate filling, which ensures that each coordinate can be estimated systematically once, and in the process of feature extraction of the data, factors such as unstable or inconspicuous presentation of the data can be effectively solved.

4. Validation of the Effectiveness of the Art Design System Module

4.1. Simulation Experiment Results

In order to verify the operation effect of the art design system proposed in this paper, comparative experiments were conducted with the traditional system. In order to guarantee that the experimental results are real and effective, the experimental environment and experimental parameters are set uniformly. The experiment uses Matlab model and SPAS/DYEMCT software to build a simulation experiment testing platform.

The effect of the signal-to-noise removal rate during the operation of the two systems was detected for five times, and the specific detection is shown in Figure 3. In the experimental detection process, the higher the signal-to-noise ratio removal rate, indicating that the system runs better. In this paper, the system signal-to-noise ratio removal rate is much higher than the traditional system, in the detection time of 100s, the average signal-to-noise ratio removal rate is 56.04% higher than the traditional system. With the increase of detection time, the overall results of the traditional system gradually show a downward trend, while the overall detection curve of this system still tends to rise steadily.

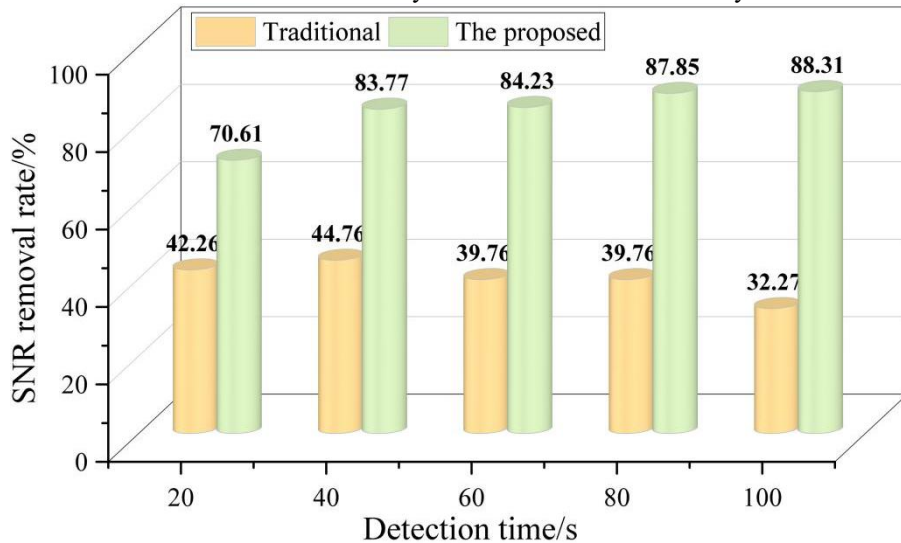


Figure 3. Effect of Signal-to-Noise Ratio Removal Rate.

4.2. Image Processing Effectiveness Analysis

Recognizing the style of an image is fundamental to understanding and appreciating visual art, including art painting classification, architectural classification, and other visual art-related abstraction tasks. The Painting91 dataset is selected for experimental testing in this chapter. This dataset provides fixed training and test set divisions and contains 1862 and 1354 images, respectively.

4.2.1. Tasks for Categorizing Painters

In this paper, we have conducted experiments on layering based on VGGNet, in which the output of the convolutional layer is directly connected to the classification layer, instead of using the fully connected layer. The modified network can be considered as a classifier, which is initialized based on different classification tasks using the network parameters of the trained VGGNet. After that, the learning rate of all the previous convolutional layers is set to zero and only the final classification layer is learned and the classification results of each convolutional layer are obtained. In order to verify the effectiveness of this paper's improved design of the art design system using image processing technology, no image processing technology is set as the control group, the image brightness equalization restoration process is carried out on the basis of the control group as the experimental group 1, and the improvement scheme proposed in this paper is the experimental group 2. For the painter classification task of the Painting91 dataset, the results of the classification accuracy of VGGNet in the different convolution layers are shown in Table 1, as shown in parentheses. For example, as shown in Table 1, the numbers in parentheses indicate the improved classification accuracy compared with the left column. The classification accuracy of experimental group 2 (the improved scheme in this paper) shows a significant incremental trend with the increase of convolutional layer depth: the conv1 layer improves by 4.38 percentage points compared with that of experimental group 1, and the improvement extends to 4.43 percentage points in the conv5_2&3 layers. The improvement of experimental group 1 is lower than that of experimental group 2, but still better than the control group.

Table 1. Comparison of classification accuracy results for painter classification tasks.

	Classification accuracy/%		
	Control group	Experimental Group 1	Experimental Group 2
conv1	20.53	24.87(4.34)	29.25(4.38)
conv2	28.65	32.75(4.10)	37.26(4.51)
conv3	37.16	41.57(4.41)	46.91(5.34)
conv4	45.68	49.33(3.65)	54.38(5.05)
conv5	51.46	55.06(3.60)	59.92(4.86)
conv5_1&2	53.93	57.98(4.05)	62.47(4.49)
conv5_1&3	57.22	61.37(4.15)	65.35(3.98)
conv5_2&3	58.09	62.49(4.40)	66.92(4.43)

4.2.2. Artistic Style Classification Tasks

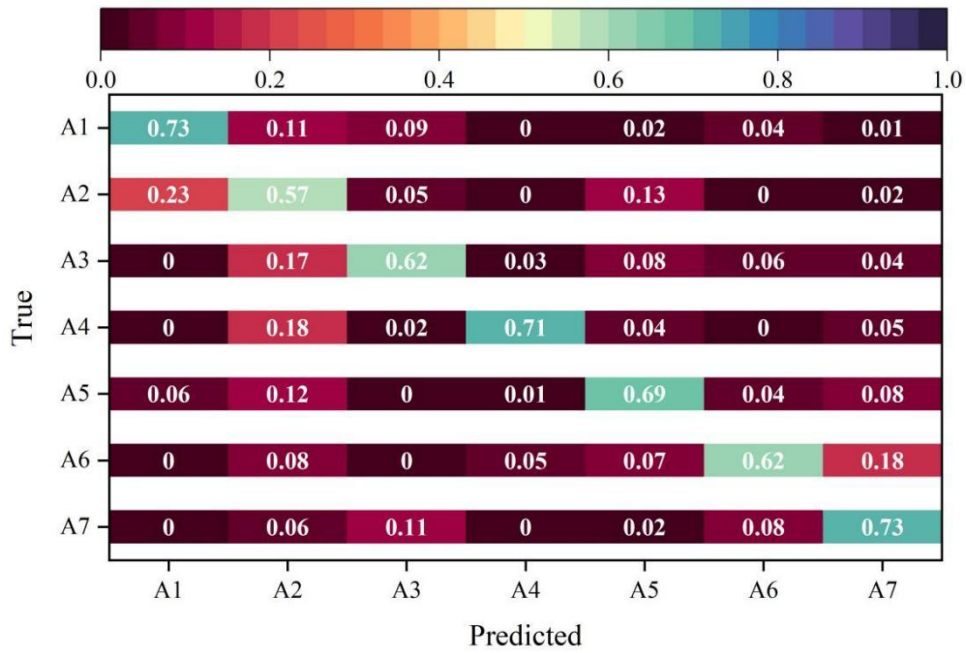
For the art style classification task in the Painting91 dataset, a comparison of the VGGNet classification accuracy results in different convolutional layers is shown in Table 2, with the numbers in parentheses indicating the improved classification accuracy compared to the left column. The classification accuracy of experimental group 2 in the conv5_2&3 layers reaches 75.36%, which is an improvement of 8.33 percentage points over the control group. The two groups of data together show that the image processing technique proposed in this paper effectively enhances the model's ability to perceive artistic details by optimizing image brightness equalization and feature fusion. And with the increase of network depth, its advantage of characterizing higher-order abstract features is further amplified, providing better quality input features for subsequent classification tasks.

Table 2. Comparison of classification accuracy results for art style classification tasks.

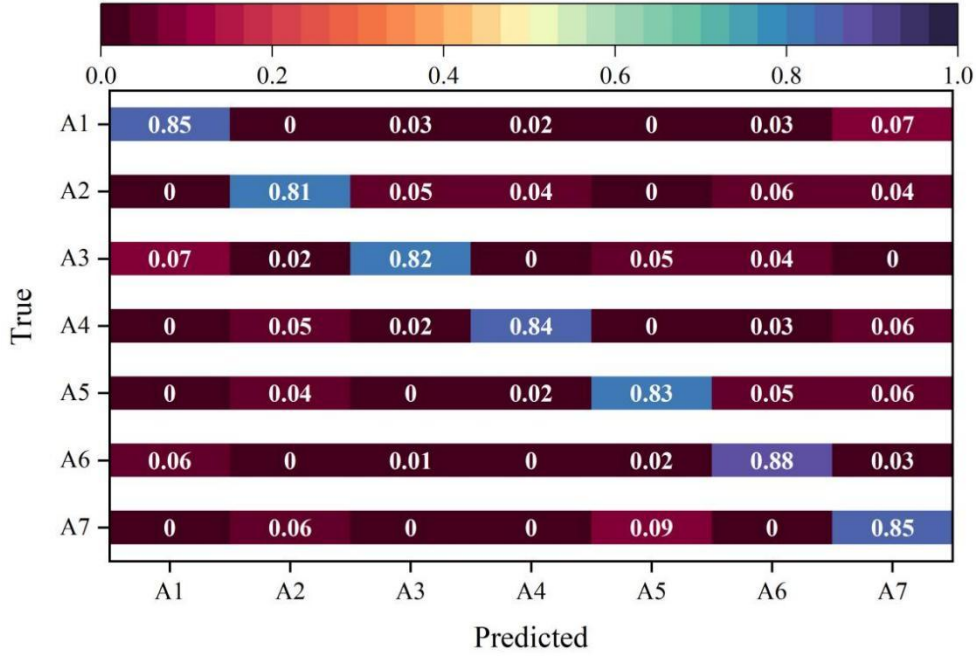
	Classification accuracy/%

	Control group	Experimental Group 1	Experimental Group 2
conv1	22.67	25.43(2.76)	30.73(5.30)
conv2	28.78	31.33(2.55)	36.84(5.51)
conv3	39.06	42.79(3.73)	47.38(4.59)
conv4	47.22	50.41(3.19)	55.12(4.71)
conv5	56.73	59.94(3.21)	64.85(4.91)
conv5_1&2	60.35	63.77(3.42)	68.38(4.61)
conv5_1&3	63.84	66.91(3.07)	71.04(4.13)
conv5_2&3	67.03	70.26(3.23)	75.36(5.10)

Numbering Abstract Expressionism, Renaissance style, Romanticism, Impressionism, Realism, Baroque style, and Symbolism as A1~A7 respectively, the results of the confusion matrix comparison between the control group and the experimental group 2 on the Painting91 style dataset are shown in Fig. 4(a~b). The method in this paper obtains a significant improvement in the accuracy of image classification in different art styles compared to the control group. Especially for the Renaissance style art paintings, the classification accuracy using this paper's method is improved by nearly 25%. This also proves the reliability of using improved image processing techniques for the recognition of visual art image styles.



(a) Control group



(b) Experimental Group 2

Figure 4. Comparison results of confusion matrices.

4.3. Analysis of the Effect of Super-Resolution Reconstruction

This chapter uses three datasets as the dataset for super-resolution model training, which involves four classification tasks for visual art images (including art paintings, sculptures, architecture, and clothing). The total number of images is divided into training, validation and test sets in the ratio of 8:1:1. Dividing the images in this way makes full use of the data for training and ensures the generalization ability of the model.

4.3.1. Experimental Results at Different Magnifications

The experiments in this paper train three image reconstruction models, 3x, 4x, and 5x, according to the different magnifications of super-resolution reconstruction, and use the dataset to test the PSNR and SSIM metrics of the reconstructed super-resolution images under the three magnifications. The models in this paper are compared with the mainstream models Bicubic, SRCNN, and SRGAN, and the experimental results are shown in Table 3. From the data in the table, it can be seen that this paper's model obtains a good improvement compared with the control model at different magnifications, and the PSNR is improved by 10.85%, 12.86%, and 14.87% at 3x, 4x, and 5x magnifications, respectively, compared with the SRGAN model, which is the second-best performer, and the SSIM reaches 0.8002, 0.7123, and 0.6251.

Table 3. Experimental results at different magnifications.

Model	Magnification factor	PSNR	SSIM
Bicubic	×3	21.08	0.7037
Bicubic	×4	19.86	0.6536
Bicubic	×5	18.77	0.5144
SRCNN	×3	23.58	0.7243
SRCNN	×4	22.05	0.6706
SRCNN	×5	20.84	0.5634
SRGAN	×3	24.42	0.7483
SRGAN	×4	23.17	0.6924

SRGAN	×5	22.06	0.6032
The proposed	×3	27.07	0.8002
The proposed	×4	26.15	0.7123
The proposed	×5	25.34	0.6251

4.3.2. Comparison of Objective Indicators

Visual art focuses on visual effects, and it involves various forms of art such as painting, sculpture, and decorative arts. The results of the comparison of the quantitative metrics of the four more representative types of images, namely art painting, sculpture, architecture and clothing, are shown in Table 4. The model in this paper shows comprehensive advantages on all types of images, with PSNR of 27.84 for the art painting category, which is 2.78 higher than the next best SRGAN. The SSIM for the sculpture, architecture, and clothing categories are improved by 0.0296, 0.0192, and 0.0187, respectively. This result shows that the super-resolution reconstruction model in this paper is extremely adaptable to different types of art images. For the high texture complexity of art paintings, it can effectively suppress the noise and retain the details; for the structural features of sculptures, it can accurately reconstruct the edge information; for the lines and proportions of buildings, it can maintain the clarity of the overall composition. For the material characteristics of clothing, delicate light and shadow changes can be restored. This cross-genre stability verifies the model's universality to diverse image needs in the art and design field.

Table 4. Comparison of different types of PSNR/SSIM.

Category	Bicubic	SRCNN	SRGAN	The proposed
Art paintings	22.43/0.7397	24.06/0.7564	25.06/0.7993	27.84/0.8108
Sculptures	19.03/0.6166	21.24/0.6418	22.48/0.6739	25.99/0.7035
Architecture	20.11/0.6735	22.85/0.6904	23.93/0.7373	26.26/0.7565
Costumes	20.04/0.6637	22.77/0.6873	23.82/0.7294	26.11/0.7481

By selecting representative samples, the performance of the model can be demonstrated and analyzed more effectively. Eight samples within the dataset are selected for the experiments, which cover different types of scenes and detailed features in the dataset and can represent the diversity and complexity of the dataset. The results of the comparison of quantitative image metrics for the eight samples are shown in Table 5. The average PSNR value of this paper's model in all 8 samples is 26.70, which is 1.84 higher than that of SRGAN, and the average value of SSIM reaches 0.7990. It shows that the model can still maintain stable reconstruction quality under various challenging scenarios, and this kind of fine validation at the sample level not only confirms the model's advantage in macro indexes, but also proves its effectiveness in the art and design classroom for the model is able to meet the students' needs for high-definition art materials. The model is able to meet the students' demand for high-definition art materials, and help improve the efficiency of classroom interaction and knowledge transfer.

Table 5. Comparison of PSNR/SSIM in different samples.

Sample	Bicubic	SRCNN	SRGAN	The proposed
1	21.49/0.7267	22.33/0.7395	24.99/0.7887	26.78/0.8003
2	21.33/0.7242	22.21/0.7388	24.67/0.7829	26.61/0.7994
3	21.85/0.7301	22.67/0.7426	25.09/0.7894	26.94/0.8018
4	22.06/0.7324	22.96/0.7433	25.27/0.7911	27.08/0.8025
5	21.03/0.7216	21.98/0.7328	24.56/0.7803	26.45/0.7962
6	21.79/0.7287	22.64/0.7371	25.01/0.7890	26.83/0.8009
7	20.98/0.7201	21.83/0.7312	24.47/0.7792	26.28/0.7937
8	21.41/0.7259	22.29/0.7386	24.86/0.7945	26.61/0.7972

4.3.3. Comparison of Subjective Evaluation Indicators

The effects of super-resolution reconstruction were compared in 20 localized images with different brightness contrasts, styles, and texture details. The subjective reconstruction quality of the images was evaluated using the MOS method. Twenty-five industry personnel were randomly invited to judge the image reconstruction effect and artistry, and the evaluation criteria were divided into two aspects: global reconstruction quality, and detail reconstruction artistry. The MOS scoring interval was set to [0,5], and the average value was calculated as the final MOS score after the statistical scoring results. The comparison results of subjective evaluation indexes under different models are shown in Figure 5. The model in this paper achieves scores of 4.67 and 4.78 in both global reconstruction quality and detail reconstruction artistry, respectively, which are better than the control model.

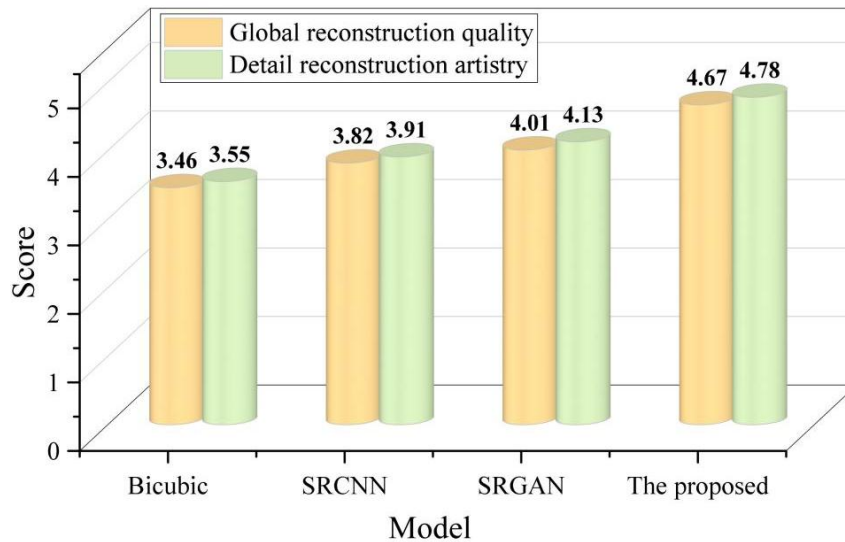


Figure 5. Comparison results of subjective evaluation indicators.

5. Conclusion

This paper centers on the innovation of art design teaching mode driven by artificial intelligence, and proves the effectiveness of the proposed art design system module through experiments.

Overall, the signal-to-noise ratio removal rate of the system in this paper is much higher than that of the traditional system, and the average signal-to-noise ratio removal rate is 56.04% higher than that of the traditional system when the detection time is 100s. With the increase of detection time, the overall results of the traditional system gradually show a downward trend, while the overall detection curve of this paper's system still tends to rise steadily.

In the painter classification task, the classification accuracy of this paper's improved scheme shows a significant incremental trend with the increase of convolutional layer depth: the conv1 layer is improved by 4.38 percentage points compared with the experimental group 1, and the enhancement amplitude is expanded to 4.43 percentage points to the conv5_2&3 layers. In the art style classification task, the classification accuracy of this paper's improved scheme in the conv5_2&3 layer reaches 75.36%, which is an improvement of 8.33 percentage points over the control group. The two sets of data together show that the image processing technique proposed in this paper provides better quality input features for the subsequent classification task by optimizing image brightness equalization and feature fusion. For the super-resolution reconstruction experiments, the PSNR of this paper's model is improved by 10.85%, 12.86%, and 14.87% under 3x, 4x, and 5x magnification, respectively, compared with the next best performing SRGAN model, and the SSIM reaches 0.8002, 0.7123, and 0.6251. The model shows comprehensive advantages on all types of images, and the fine validation at the sample level proves that it has a good advantage in the super-resolution reconstruction capability of real teaching materials in art and design classroom. In the subjective evaluation, the model scores 4.67 and 4.78 in global reconstruction quality and detail reconstruction artistry, respectively, which are better than the control model.

References

1. Wang, Z. (2022, February). Intersection and integration: interdisciplinary design practice and new media art design teaching. In 2021 Conference on Art and Design: Inheritance and Innovation (ADII 2021) (pp. 271-275). Atlantis Press.

2. Cross, N. (2018). Developing design as a discipline. *Journal of Engineering Design*, 29(12), 691-708.
3. Henriksen, D. (2017). Creating STEAM with design thinking: Beyond STEM and arts integration. *The STEAM Journal*, 3(1), 11.
4. Zwirn, S. G., & Vande Zande, R. (2017). Differences between art and design education—or differences in conceptions of creativity?. *The Journal of Creative Behavior*, 51(3), 193-203.
5. Bryukhanova, H., Cherniavskyi, K., Udriș, I., Marchenko, A., & Bielofastova, T. (2021). The modernization of future specialists' professional training in the field of advertising design in higher education institutions. *Revista on line de Política e Gestão Educacional*, 2694-2709.
6. Meyer, M. W., & Norman, D. (2020). Changing design education for the 21st century. *She Ji: The Journal of Design, Economics, and Innovation*, 6(1), 13-49.
7. Radha, R. K. (2022). Flexible smart home design: Case study to design future smart home prototypes. *Ain Shams Engineering Journal*, 13(1), 101513.
8. Bitterman, N., & Shach-Pinsly, D. (2015). Smart home—a challenge for architects and designers. *Architectural science review*, 58(3), 266-274.
9. Chamoso, P., González-Briones, A., Rodríguez, S., & Corchado, J. M. (2018). Tendencies of technologies and platforms in smart cities: a state-of-the-art review. *Wireless Communications and Mobile Computing*, 2018(1), 3086854.
10. Peng, J. (2020). Intelligent technology-based improvement of teaching ability of professional courses in art design. *International Journal of Emerging Technologies in Learning (Ijet)*, 15(23), 193-207.
11. Fang, F., & Jiang, X. (2024). The analysis of artificial intelligence digital technology in art education under the internet of things. *IEEE Access*, 12, 22928-22937.
12. Lin, Y., Cai, L., & Yang, N. (2025). Research on the Path of AIGC Assisted Art Design Creation for Non Art Design Majors. In *International Conference on Human-Computer Interaction* (pp. 68-87). Springer, Cham.
13. Xu, J. (2024). Exploration of the Applications of Image-based AIGC in Art Education. *Advances in Social Development and Education Research*, 1(3), 60-65.
14. Wang, Q., Li, C., & Zhu, L. (2024). Analysis on the acceptance of AIGC technology by art and design students in universities in China. *ABAC Journal*, 44(4), 218-235.
15. Chiang, I., Lin, P. H., & Lin, R. (2025). AIGC-Driven Innovative Design Education Based on Material Experience and Cultural Context. In *International Conference on Human-Computer Interaction* (pp. 3-17). Springer, Cham.
16. Knochel, A. D., & Patton, R. M. (2015). If art education then critical digital making: Computational thinking and creative code. *Studies in Art Education*, 57(1), 21-38.
17. Wang, S. (2020, October). Smart Education—The necessity and prospect of big data mining and artificial intelligence technology in art education. In *Journal of Physics: Conference Series* (Vol. 1648, No. 4, p. 042060). IOP Publishing.
18. Zhu, Z. T., Yu, M. H., & Riezebos, P. (2016). A research framework of smart education. *Smart learning environments*, 3, 1-17.
19. Hwang, G. J., Xie, H., Wah, B. W., & Gašević, D. (2020). Vision, challenges, roles and research issues of Artificial Intelligence in Education. *Computers and Education: Artificial Intelligence*, 1, 100001.
20. Choi, S. K., DiPaola, S., & Töyrylä, H. (2021). Artistic style meets artificial intelligence. *Journal of Perceptual Imaging*, 4, 1-14.
21. Lin, Y. (2020, October). Research on application and breakthrough of artificial intelligence in art design in the new era. In *Journal of Physics: Conference Series* (Vol. 1648, No. 3, p. 032187). IOP Publishing.
22. Wu, J., Cai, Y., Sun, T., Ma, K., & Lu, C. (2024). Integrating AIGC with design: dependence, application, and evolution—a systematic literature review. *Journal of Engineering Design*, 1-39.
23. Zhang, B., & Romainoor, N. H. (2023). Research on artificial intelligence in new year prints: the application of the generated pop art style images on cultural and creative products. *Applied Sciences*, 13(2), 1082.
24. Yu, L., & Zheng, Q. (2023). AI-Enhanced Digital Creativity Design: Content-Style Alignment for Image Stylization. *IEEE Access*, 11, 143964-143979.
25. Bhangale, K. B., Desai, P., Banne, S., & Rajput, U. (2022, May). Neural style transfer: reliving art through artificial intelligence. In *2022 3rd International Conference for Emerging Technology (INCET)* (pp. 1-6). IEEE.
26. Feng, J., & Wang, Z. (2024). Art Design Style Mining Based on Deep Learning and Data Mining. *Computer-Aided Design and Applications*, 33-47.
27. He, J. (2024). A Study on the Influence of Artificial Intelligence on Image Art Design. In *SHS Web of Conferences* (Vol. 181, p. 04028). EDP Sciences.
28. Wang, Y., Xi, Y., Liu, X., & Gan, Y. (2024). Exploring the dual potential of artificial intelligence-generated content in the esthetic reproduction and sustainable innovative design of ming-style furniture. *Sustainability*, 16(12), 5173.